

# Spectroscopy and dynamics of mixtures of water with acetone, acetonitrile, and methanol

Dean S. Venables and Charles A. Schmuttenmaer

*Department of Chemistry, Yale University, 225 Prospect Street, P.O. Box 208107,  
New Haven, Connecticut 06520-8107*

(Received 25 July 2000; accepted 2 October 2000)

Binary mixtures of water with acetone, acetonitrile, and methanol over their entire range of compositions have been studied spectroscopically and by using molecular dynamics (MD) simulations. We report absorption coefficients and indices of refraction over a frequency range from 3 to 55  $\text{cm}^{-1}$ , and from 400 to 1200  $\text{cm}^{-1}$ . The far-infrared absorption of the mixtures is substantially less than that for ideal mixtures, and Debye time constants calculated from the spectra are longer for the real than for the ideal mixtures. Significant composition dependence is observed in the high frequency librational spectra of the mixtures, and is reproduced by the MD simulations. Single dipole and angular velocity spectra are also reported, as are detailed changes in the hydrogen bonding environment in the mixtures. There is a loss of tetrahedral water structure on mixing, yet water molecules have a strong tendency to aggregate, especially in the acetone and acetonitrile mixtures. Spatial distribution functions are reported for the acetone/water system. © 2000 American Institute of Physics. [S0021-9606(00)52148-5]

## I. INTRODUCTION

The obvious importance of water as a solvation medium has fueled a tremendous effort to understand the properties of aqueous solutions. Adding to the scientific interest in water are its peculiarities as a solvent—namely, its effectiveness in solvating ionic and dipolar substances, and its poor ability to solvate nonpolar molecules (“the hydrophobic effect”). These properties of water have a large bearing on biological systems and other chemical systems of practical importance, and are related to the highly associating nature of water through its ability to form hydrogen bonds. We shall restrict our attention in this article to binary mixtures of water with acetone, acetonitrile, and methanol, all of which have large dipole moments.

One of the central issues in understanding solvation is the degree to which the dynamics of molecules in mixtures differs from that in the neat liquids. It has been known for some time that the dynamics of aqueous mixtures are considerably slower than those of neat water.<sup>1</sup> The effect of the co-solvent on the hydrogen bonding environment in the mixture and the distribution of molecules of either species throughout the mixture are also important questions. The structure and the dynamics of the mixtures are clearly related. Thus, the slowing of the dynamics of aqueous mixtures has usually been explained in terms of an enhancement in the water structure, for instance, in the famous “iceberg hypothesis” of Frank and Evans.<sup>2</sup> Self-aggregation of water or its co-solvent molecules is a commonly invoked explanation for some of the properties of aqueous mixtures.<sup>1,3,4</sup> The effects of different co-solvents on the dynamics and structure of water is also of interest. In the mixtures considered in this article, methanol is expected to affect water differently from acetone and acetonitrile, since methanol is an associating liquid that can both donate and accept hydrogen bonds, whereas

acetone and acetonitrile can only accept hydrogen bonds.

The low frequency spectra are essential to understanding the dynamics of liquids, because they are indicative of rotational, translational, and librational motions. In hydrogen bonding liquids such as water and methanol, the broad absorption band around 700  $\text{cm}^{-1}$  is particularly interesting because it arises from librational motions involving mainly the hydrogen atoms of the molecule.<sup>5</sup> It is therefore sensitive to the hydrogen bonding environment in the liquid. Regrettably, there are almost no experimental spectra of dipolar liquid mixtures below about 800  $\text{cm}^{-1}$ —that is, in lower frequency infrared (IR) and the far-infrared (far-IR) regions of the spectrum. This is because there are few intense broad-band sources of radiation at low frequencies and because hydrogen bonding liquids absorb strongly in this region.<sup>6–9</sup>

The interpretation of low frequency liquid spectra, when available, is not straightforward. The complexity of the many-bodied interactions and the heterogeneous environment experienced by the molecules in a liquid is not amenable to a simple analytical description. Exceptions are the Debye and related models, which describe the reorientation of molecules in the microwave and far-IR regions of the spectrum. Analytical techniques do not give a detailed molecular description of the liquid, however, and the most promising method of interpreting the spectra is via molecular dynamics (MD) simulations.

Knowledge of the microscopic details of liquids has been greatly expanded by computer simulations (e.g., see Refs. 5 and 10). Simulations of neat liquids have accurately predicted many of the properties of liquids, including thermodynamic and structural properties, and dynamical behavior. The agreement between the simulated and the experimental results gives us confidence that the simulations are accurately modeling the molecular details of the liquid. Mix-

tures of liquids can likewise be simulated by using the interaction potentials of the neat liquids. However, it is not necessarily the case that the effective pair potentials, which were parametrized to describe the properties of neat liquids, will accurately predict the properties of mixtures. In particular, it is known that the Lorentz–Berthelot combining rules for describing the cross-potentials of Lennard-Jones interactions tend to underestimate the interactions of unlike species.<sup>11</sup> These concerns notwithstanding, simulations of mixtures have been reasonably successful in predicting mixture properties.<sup>11</sup> Nevertheless, it remains an important task to compare experimental and predicted properties of the mixtures.

We have recently shown that spectra from MD simulations give quite reasonable agreement with the experimental spectra of methanolic mixtures.<sup>6,7</sup> The experimental and computed spectra both show a marked red-shift in the high frequency librational band of methanol as the methanol concentration decreases. This red-shift was attributed to increased hydrogen bonding between methanol and its co-solvent. Skaf has also predicted large changes in the absorption band of water in dimethyl sulfoxide (DMSO)/water mixtures.<sup>12</sup>

In this article, we extend our work to the more important case of aqueous mixtures, and will examine binary mixtures of water with acetone, acetonitrile, and methanol. We find that acetone and acetonitrile cause a large red-shift in the librational band of water, whereas the same band only undergoes a slight blue-shift in methanol/water mixtures. These trends are reproduced by the MD simulations. In the far-IR, all the aqueous mixtures show a substantial decrease in absorption, which is attributed to a slowing of the rotational dynamics of the mixtures. The hydrogen bonding environment in the mixtures is also examined in more detail than has been done previously.

In Sec. II, previous work on the mixtures studied here is discussed, and experimental details of our work are described in Sec. III. The results are presented in Sec. IV: first, the experimental far-IR and IR spectra are presented, followed by the spectra, hydrogen bonding information, and spatial distribution functions (SDFs) of the simulations. The results are discussed more broadly in Sec. V and summarized in Sec. VI.

## II. BACKGROUND

Experimental measurements of the dynamics of acetone/water, acetonitrile/water, and methanol/water mixtures indicate a considerable decrease in the mobility of the mixtures. Thus, microwave dielectric relaxation measurements of acetone/water mixtures show a broad maximum in the Debye relaxation time constant,  $\tau_D$ , from 0.2 to 0.6 volume fraction acetone,<sup>13,14</sup> which corresponds to the maximum in the viscosity of the mixtures at 0.5 volume fraction acetone.<sup>1</sup> Correlation times determined by nuclear magnetic resonance (NMR) also have large maxima at these compositions.<sup>1</sup> Measures of molecular mobility in acetonitrile/water mixtures based on NMR correlation times,<sup>1</sup> diffusion measurements,<sup>1</sup> and Debye relaxation times<sup>8</sup> also indicate a slowing of the mixture dynamics. The slower dynamics have been attrib-

uted to an increase in the water structure, and microheterogeneity has been proposed in the system.<sup>1</sup> Previous studies of acetonitrile/water mixtures have been reviewed in greater detail in earlier work.<sup>8</sup>

In contrast, the Debye relaxation times of methanol/water mixtures do not have a maximum relative to the neat liquids,<sup>15–17</sup> although the diffusion coefficients<sup>18</sup> and NMR correlation times do indicate a significant slowing of the dynamics in the middle of the composition range.<sup>1</sup> The relaxation time constant from depolarized Raleigh light scattering, which is related to hydrogen bond breaking and formation, has a maximum at 0.5 volume fraction methanol.<sup>19</sup>

We have already reviewed some of the MD simulations of neat liquids,<sup>7</sup> and here shall focus instead on the mixtures. In acetone/water mixtures, the radial distribution functions (RDFs) associated with hydrogen bonding between water molecules increase enormously with dilution of water, which was attributed to an increase in the water structure in the mixtures. Both the water–water and water–acetone hydrogen bond lifetimes increase with dilution of water.<sup>20</sup>

Kovacs and Laaksonen have shown that there is also a large increase in the water–water RDFs in acetonitrile/water mixtures.<sup>4</sup> RDFs between acetonitrile-acetonitrile sites are unaffected by mixing except at water-rich compositions. The RDFs suggest microheterogeneity, and at low water concentrations dimers, trimers, and tetramers of water are favored over monomeric water molecules. Oscillations in the linear velocity autocorrelation functions (ACFs) are damped by the addition of acetonitrile, indicating a breakdown of the water structure. The high frequency librations of water are shifted to lower frequencies and become narrower at high concentrations of acetonitrile. However, small amounts of acetonitrile cause a blue-shift of the water libration, indicating a slight enhancement of structure.

Mixtures of methanol and water have received a great deal of attention,<sup>5,20–26</sup> and only some key results will be presented here. The addition of either methanol to water, or water to methanol, results in the solute adopting some of the structure and hydrogen bonding character of the solvent.<sup>21,22</sup> Water molecules at low concentrations tend to aggregate together more than expected for random mixing, whereas when methanol is dissolved in water it is unlikely to have other methanol molecules in its solvation shell.<sup>20–24</sup> Methanol molecules are not efficiently incorporated into the water structure.<sup>25</sup>

The static and dynamic dielectric properties of methanol/water mixtures have been extensively investigated by Ladanyi and co-workers.<sup>23,25,27</sup> They found that interspecies cross-correlations have a significant impact on the dipolar time correlation functions (TCFs). The high frequency librational band broadens with water content.<sup>23</sup> Pálkás *et al.* have shown that the librational frequencies are higher for methanol molecules with a greater number of hydrogen bonds, and that the linewidths of the librational band are narrower in methanol-rich mixtures.<sup>26</sup> The velocity ACFs of the water and methanol hydrogen atoms change upon mixing, with the water ACFs becoming more oscillatory and the methanol ACFs slowing slightly.<sup>20</sup>

TABLE I. The number of molecules of the non-water component used in the simulations. The densities of acetone/water (Ref. 39), acetonitrile/water (Ref. 40), and methanol/water (Ref. 41) mixtures are given, as are the corresponding compositions of the mixture (in volume fractions).

Acetone/water			Acetonitrile/water			Methanol/water		
No. AT	Density (g cm <sup>-3</sup> )	V <sub>AT</sub>	No. AN	Density (g cm <sup>-3</sup> )	V <sub>AN</sub>	No. ME	Density (g cm <sup>-3</sup> )	V <sub>ME</sub>
0	0.9971	0.0000	0	0.9971	0.0000	0	0.9971	0.0000
6	0.9873	0.1046	8	0.9843	0.1008	10	0.9830	0.0985
16	0.9704	0.2465	22	0.9603	0.2484	28	0.9619	0.2511
42	0.9294	0.4968	55	0.9070	0.4989	66	0.9237	0.4977
91	0.8700	0.7486	110	0.8437	0.7515	123	0.8670	0.7486
149	0.8225	0.9009	163	0.8038	0.8996	173	0.8233	0.9006
178	0.8063	0.9504	187	0.7915	0.9495	...	...	...
195	0.7968	0.9743	201	0.7843	0.9750	...	...	...
216	0.7851	1.0000	216	0.7766	1.0000	216	0.7865	1.0000

### III. EXPERIMENT

#### A. Infrared and far-infrared spectra

Infrared and far-IR spectra were recorded at room temperature (18 °C to 21 °C). Methanol, acetonitrile, and acetone (all greater than 99.5% purity) were obtained from Baker and were used as received. They were mixed with deionized water, following the procedure described previously,<sup>6,8</sup> to form binary mixtures of 0.10, 0.25, 0.50, 0.75, and 0.90 by volume fraction. The uncertainty in the volume fractions of the mixtures is estimated to be less than 0.002. The volume fraction of component *i* is denoted by the symbol  $V_i$ ; where appropriate, we use mole fractions designated by the conventional symbol  $x_i$ . The component *i* may be written as AT for acetone, AN for acetonitrile, ME for methanol, or WA for water. The use of volume fraction in preference to mole fraction when interpreting spectra has already been discussed.<sup>6,8</sup>

A generic transmission Fourier-transform infrared (FTIR) spectrometer (Midac M1200) was used to measure spectra of the liquids in the mid-IR region. Samples were held in a custom-designed variable pathlength cell.<sup>6</sup> The ability to make changes of 0.5  $\mu\text{m}$  in the pathlength is essential for accurate measurement of intense absorption bands. Spectra were measured over a range of pathlengths and the absorption coefficients were calculated using Beer's law. In this manner, absorption coefficients of the liquids were determined for frequencies above 400  $\text{cm}^{-1}$ . An artifact in the spectra between 715 and 735  $\text{cm}^{-1}$  is sometimes present and is caused by an absorption band of the polyethylene bag. Our results are in quantitative agreement with those of Bertie for neat methanol<sup>28</sup> and water.<sup>29</sup> Highly absorbing samples (i.e., those with a high concentration of water) are significantly more noisy than others, however.

Far-IR spectra were measured using femtosecond terahertz (fs-THz) pulse spectroscopy.<sup>30</sup> Intense subpicosecond far-IR pulses, with frequency components from 0.1 to about 4 THz (3 to 133  $\text{cm}^{-1}$ ), are propagated through samples of variable thickness. The amplitude of the pulse in the time domain is mapped out by varying the arrival time of a visible gating pulse relative to that of the THz pulse at a suitable detector. The time-domain spectrum is Fourier transformed to yield the frequency-domain power spectrum and phase

delay. The spectrometer and the data acquisition procedure have been described in earlier work, and we have demonstrated that this technique is well suited to measuring far-IR spectra of highly absorbing liquids.<sup>6,8,9</sup> Our spectra cover from 5  $\text{cm}^{-1}$  up to 60  $\text{cm}^{-1}$ .<sup>31</sup> Because both the absorption coefficient and the index of refraction are determined, the complex-valued dielectric constant can also be calculated without a Kramers–Kronig analysis. The far-infrared and infrared data for all the mixtures have been archived in the EPAPS repository.<sup>32</sup>

#### B. Molecular dynamics simulations

Molecular dynamics simulations under constant volume conditions were carried out using the MolDy program.<sup>33</sup> Systems of 216 rigid molecules were simulated using periodic boundary conditions at an average temperature of 298 K, which was maintained using a Nosé–Hoover thermostat.<sup>34</sup> The effective pair potentials were OPLS for methanol<sup>35</sup> and acetone,<sup>36</sup> Jorgensen-Briggs for acetonitrile,<sup>37</sup> and TIP4P for water.<sup>38</sup> Spectra from the simulations did not appear to be particularly sensitive to the potentials chosen. Long-range electrostatic interactions were treated by Ewald summation. After an initial equilibration period, data were collected over an additional 126 ps, where the integration time step of the simulations was 0.7 fs. Dynamical quantities for the time correlation functions were output every 7 fs and the configuration of the system was output every 70 fs. The densities,<sup>39–41</sup> volume fractions, and number of molecules in each simulation are listed in Table I.

The equilibration of the mixtures was followed by monitoring the RDFs as well as the fraction of molecules of each species that had a given number of hydrogen bonds. For the simulations presented here, the equilibration period of methanol/water mixtures was 112 ps, and that for acetone/water and acetonitrile/water was at least 154 ps. Some compositions with low water concentrations required significantly longer equilibration times.<sup>42</sup>

The far-IR spectra of the simulated liquids were calculated from the ACF of the total dipole moment,  $\mathbf{M}(t)$ , using the equation

$$\alpha(\omega)n(\omega) = \frac{4\pi\omega \tanh(\hbar\omega/2kT)}{3\hbar cV} \times \int_{-\infty}^{+\infty} e^{-i\omega t} \langle \mathbf{M}(t) \cdot \mathbf{M}(0) \rangle dt, \quad (1)$$

where  $\alpha$  is the absorption coefficient and  $n$  is the index of refraction at an angular frequency,  $\omega$ , of a sample of volume,  $V$ , and temperature,  $T$ .<sup>43</sup> The absorption coefficient and index of refraction from the simulations were separated by a Kramers–Kronig analysis.<sup>44–46</sup>

Our approach in this work has been to calculate the total dipole of the system based on the permanent dipole of each molecule. Induced dipoles were not taken into account. We have found that simulations of nonaqueous mixtures based on this method give reasonable agreement with experiment.<sup>7</sup> The same approach has been used by Ladanyi and co-workers to study mixtures of water and methanol,<sup>23</sup> and by Skaf to study mixtures of DMSO and water.<sup>12</sup> Not incorporating the induced dipoles in the simulation is unlikely to affect the molecular motions of the liquid significantly,<sup>47</sup> although motions that do not affect the system dipole (such as translations) will not contribute to the calculated spectra. The effect of interference between the permanent and the induced dipoles, which may contribute significantly to the spectra,<sup>43,47</sup> will also not be visible. Nevertheless, the permanent dipole is the largest contributor to the spectral density and should be broadly representative of motions occurring in the liquid, particularly as the induced dipoles have much the same dielectric relaxation as the permanent dipoles.<sup>23</sup>

## IV. RESULTS

### A. Far-infrared spectra

Absorption coefficients of the mixtures are shown in Fig. 1. Indices of refraction (not shown) of the mixtures were also determined. The signal-to-noise ratios of the spectra decrease rapidly above 50  $\text{cm}^{-1}$ , owing to a sharp drop in the intensity of high frequency components of the pulse, and to the high absorption of the samples. The error bars are generally small enough to distinguish between spectra of similar compositions. Figure 2 shows the composition dependence of the experimental values of the optical constants at selected frequencies, together with that of the ideal values<sup>6</sup>

$$\alpha_{\text{ideal}}(\omega) = \rho_{\text{real}}/\rho_{\text{ideal}}[V_1\alpha_1(\omega) + V_2\alpha_2(\omega)] \quad (2)$$

and

$$n_{\text{ideal}}(\omega) = \rho_{\text{real}}/\rho_{\text{ideal}}[V_1n_1(\omega) + V_2n_2(\omega)], \quad (3)$$

where  $\alpha_i$  and  $n_i$  are the absorption coefficient and refractive index of component  $i$ . The ratio of the real and ideal densities ( $\rho_{\text{real}}$  and  $\rho_{\text{ideal}}$ ) accounts for small nonidealities in the volume of mixing.

The above spectra indicate that mixtures of water with other dipolar liquids absorb substantially less than that expected of ideal behavior. The indices of refraction also tend to be lower than ideal, especially at low frequencies. The decrease in the optical constants of mixtures in the far-IR has been observed previously in the acetonitrile/water system,<sup>8</sup> but is more pronounced in acetone/water and methanol/water

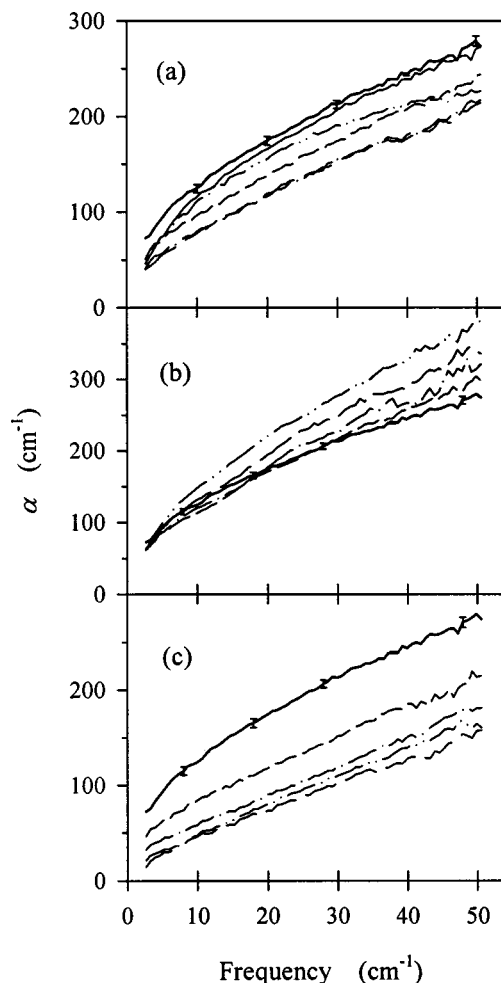


FIG. 1. The far-IR absorption coefficients of (a) acetone/water, (b) acetonitrile/water, and (c) methanol/water mixtures. The compositions (in terms of the volume fraction of water) are 0.00 (dash-dot-dotted line), 0.25 (short dashes), 0.50 (dash-dotted line), 0.75 (long dashes), and neat water (solid line). Representative error bars are shown for the spectrum of neat water.

mixtures. The difference between the ideal and the real absorption coefficients increases with frequency up to about 20  $\text{cm}^{-1}$ , above which it remains fairly constant, and nonidealities in the index of refraction drop off rapidly with frequency for all three mixtures.

The spectra of the mixtures can be related to the dynamical behavior of the liquids through the complex-valued dielectric constant,  $\hat{\epsilon} = \epsilon' - i\epsilon''$ . The components of  $\hat{\epsilon}$  are calculated from the absorption coefficients and indices of refraction using  $\epsilon' = n^2 - k^2$  and  $\epsilon'' = 2nk$ , where  $k = \alpha c/(2\omega)$ . The dielectric behavior of the mixtures was then fit to various dynamical models of the dielectric relaxation. We found that the double-Debye model gave the best fit to the data.<sup>48,49</sup> The Debye model yields the relaxation time of the sample and is given by

$$\hat{\epsilon}(\omega) = \epsilon_{\infty} + \sum_{j=1}^n \frac{\epsilon_j - \epsilon_{j+1}}{1 + i\omega\tau_j}, \quad (4)$$

where for  $n$  relaxation processes,  $\epsilon_1$  is the static dielectric constant,  $\epsilon_j$  are intermediate values of the dielectric constant,



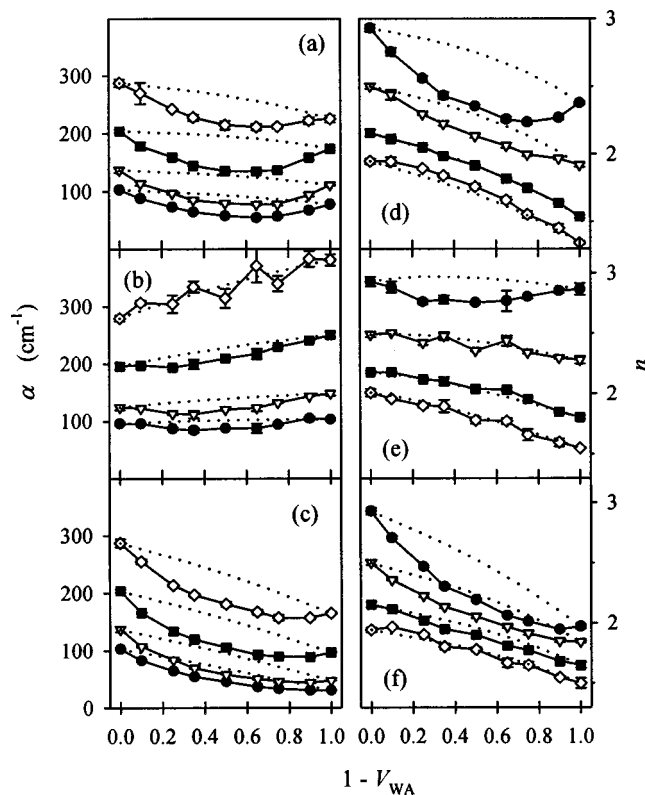


FIG. 2. Comparison of the optical constants of the mixtures with the ideal values (dotted lines) as a function of composition. (a)–(c) are the absorption coefficients; indices of refraction are shown in (d)–(f). The mixtures are acetone/water (top), acetonitrile/water (middle), and methanol/water (bottom). The frequencies shown are  $5\text{ cm}^{-1}$  (filled circles),  $10\text{ cm}^{-1}$  (open triangles),  $25\text{ cm}^{-1}$  (filled squares), and  $50\text{ cm}^{-1}$  (open diamonds).

$\epsilon_{n+1} = \epsilon_{\infty}$  is its limiting value at high frequency, and  $\tau_j$  are the relaxation time constants. Values for the static dielectric constant were determined by linear interpolation of literature results to our compositions.<sup>50,51</sup> Relaxation times were determined from fits of the double-Debye model to the experimentally determined  $\hat{\epsilon}$ . Ideal relaxation times were obtained by fitting the same model to the ideal values of the optical constants [Eqs. (2) and (3)]. The time constant associated with the slow relaxation process,  $\tau_1$ , is shown in Fig. 3. Because the uncertainties in the  $\tau_2$  values are quite large, we shall discuss only the slower relaxation times.

All three systems investigated show an appreciable increase in the slow relaxation times of the real mixtures above those of the ideal mixtures. Literature values from microwave work are included in Fig. 3 for comparison. Our results for the acetone/water mixtures show the same trend and magnitude as the values of Kumbharkhane *et al.*<sup>13</sup> The higher temperature ( $25\text{ }^{\circ}\text{C}$ ) of their experiments is partly responsible for the slightly shorter relaxation times that they report. The relaxation times of acetonitrile/water mixtures have been discussed previously.<sup>8</sup>

Our relaxation times for neat methanol and methanol-rich mixtures are lower than those reported in the literature because we have used two relaxation processes to describe the methanol relaxation, whereas three relaxation processes have been identified.<sup>15–17</sup> Our data measure the high frequency end of dielectric relaxation, and cannot distinguish

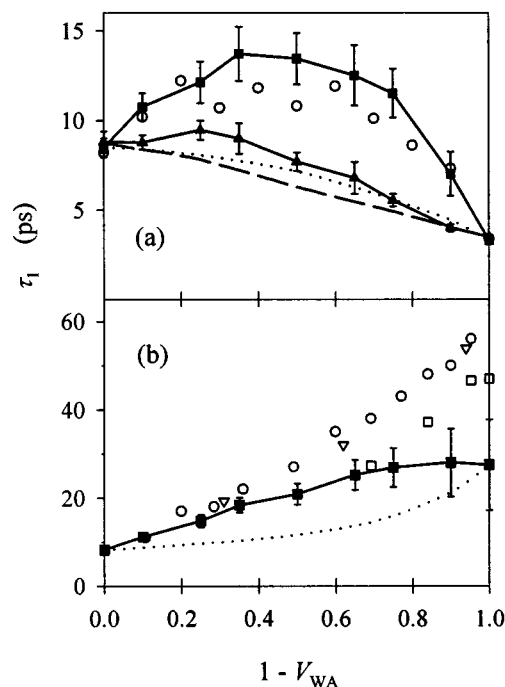


FIG. 3. The slow Debye time constants of (a) the acetone/water (filled squares) and acetonitrile/water (filled triangles) mixtures, and (b) the methanol/water mixtures (filled squares). The time constants based on the ideal optical constants are shown as a dotted line for the acetone/water and methanol/water systems, and as a dashed line for water/acetonitrile mixtures. Literature data for acetone/water mixtures are from Kumbharkhane at  $25\text{ }^{\circ}\text{C}$  (open circles) (Ref. 13). For the methanol/water system, our data are compared to microwave data from Bertolini ( $30\text{ }^{\circ}\text{C}$ ) (Ref. 15), Mashimo ( $23\text{ }^{\circ}\text{C}$ ) (Ref. 16), and Kaatz ( $25\text{ }^{\circ}\text{C}$ ) (Ref. 17) shown as open squares, open circles, and open triangles, respectively.

between multiple slow relaxation processes. The values that we obtain should therefore be regarded as *effective* relaxation times, which we use to draw out differences between the real and ideal relaxation times. With this caveat in mind, the relaxation times in methanol/water mixtures are also observed to be slower than those of the ideal mixtures.

## B. Infrared spectra

Infrared spectra of the mixtures spanning from  $400$  to  $1000\text{ cm}^{-1}$  are shown in Fig. 4. Our interest is in the effect of mixing on the broad absorption band, which arises from high frequency librations in hydrogen bonding liquids. The narrow, intramolecular features that are apparent in the acetone and acetonitrile spectra will therefore not be considered. A cursory inspection of the spectra reveals that the absorption band in acetone/water and acetonitrile/water mixtures shifts to significantly lower frequencies on mixing. This effect is similar to that seen on mixing acetone and acetonitrile with methanol.<sup>6</sup> In contrast, the position of the absorption band does not change much in methanol/water mixtures.

The position, amplitude, and width of the absorption band were determined quantitatively by fitting the absorption to a Gaussian curve.<sup>52</sup> Ideal spectra of the mixtures were likewise examined.<sup>53</sup> The amplitudes of the fitted curves changed linearly with composition. The fitted values of the peak position and width are shown in Fig. 5 as a function of composition. The extent of the red-shift—almost  $150\text{ cm}^{-1}$

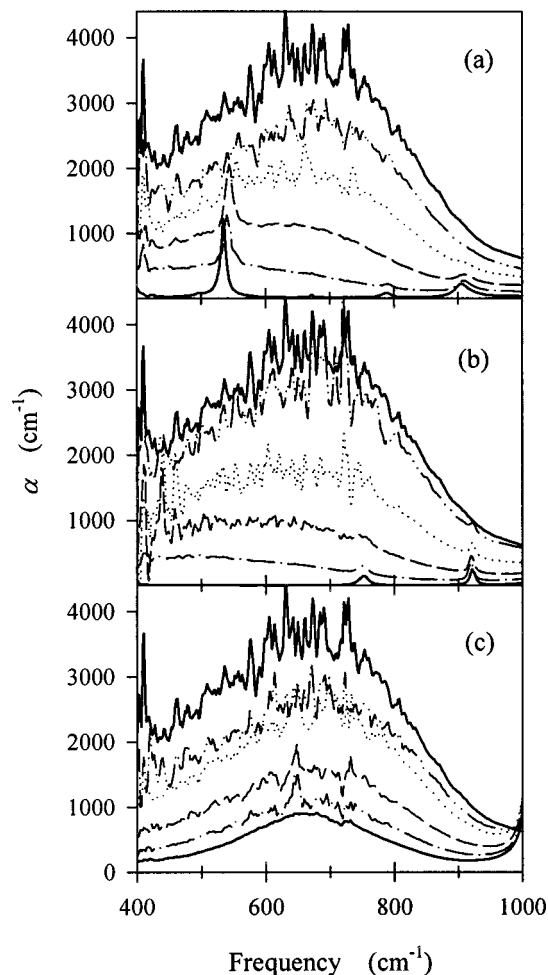


FIG. 4. The infrared spectra of (a) acetone/water, (b) acetonitrile/water, and (c) methanol/water mixtures. The neat liquids are shown as bold curves, and thin lines indicate water volume fractions of 0.75 (dash-dot-dotted lines), 0.50 (dots), 0.25 (dashes) and 0.10 (dash-dotted lines).

for acetone and  $200\text{ cm}^{-1}$  acetonitrile—is very large compared to the peak position of the neat liquid ( $670\text{ cm}^{-1}$ ). However, moderate amounts of co-solvent ( $V_{\text{WA}} > 0.7$ ) actually induce a small blue-shift in the librational band. In the methanol/water mixtures, the high frequency band is caused by the librations of both water and methanol molecules, which occur at about the same frequency. The peak position in this system remains slightly blue-shifted relative to the ideal mixture for most of the composition range.

The peak widths of the absorption band in the mixtures show consistent trends with composition, although the uncertainties are larger than those of the peak positions. In the acetone and acetonitrile mixtures, the peak width does not change appreciably before about  $V_{\text{WA}} = 0.50$ . Further dilution of water broadens the absorption band, particularly in acetonitrile/water mixtures. In methanol/water mixtures, the peak is slightly broader than expected of ideal behavior.

### C. Molecular dynamics simulations

#### 1. Spectra

Time correlation functions and the corresponding spectra of the total dipole moment, the single molecule dipole mo-

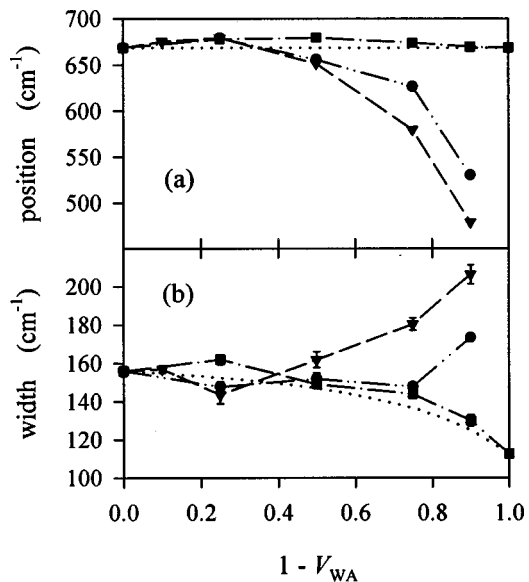


FIG. 5. The variation of the fitted (a) peak position and (b) width with composition. Circles, triangles, and squares designate acetone/water, acetonitrile/water, and methanol/water mixtures, respectively. The position and width for ideal methanol/water mixtures are shown as a dotted line.

ments, and the linear and angular velocities of each species were calculated. Only spectra of the total dipole moment are experimentally accessible. It is apparent that the shifts in the spectral density of the experimental spectra are also present in the simulated spectra of the collective dipole moment (Fig. 6). At high concentrations of acetone or acetonitrile, a greater proportion of the absorption occurs at lower frequencies. In methanol/water mixtures, on the other hand, the absorption maximum is blue-shifted relative to the spectra of the neat liquids.

The composition dependence of the absorption peak and width was quantified by calculating the first moment and the standard deviation of the spectra between  $300$  and  $950\text{ cm}^{-1}$  (Fig. 7). The composition dependence of the first moment is more modest than that of the experimental peak position for acetone and acetonitrile mixtures. Nonetheless, the key features of the spectra of these mixtures—the slight blue-shift at low co-solvent concentrations and the sharp red-shift at low water concentrations—are both evident. The standard deviations of these mixtures are not significantly affected by composition, whereas the experimental absorption of acetonitrile/water mixtures shows some broadening at low water content.

The calculated spectrum of neat methanol has a maximum at about  $50\text{ cm}^{-1}$  lower than that of neat water, whereas the absorption maxima in the experimental spectra of the neat liquids are at about the same frequency. The first moments of the ideal spectra [Eq. (2)] are slightly lower than those of the simulated spectra. The spectra is also slightly broader than expected for ideal mixtures. These small but consistent deviations from ideality are similar to those observed in the experimental spectra (Fig. 5), and agree with the observations of Ladanyi and Skaf.<sup>23</sup>

Changes in the single dipole ACFs are demonstrated by the single particle relaxation times,  $\tau_S$ , of the mixtures (Fig. 8). The relaxation time for each species is determined by

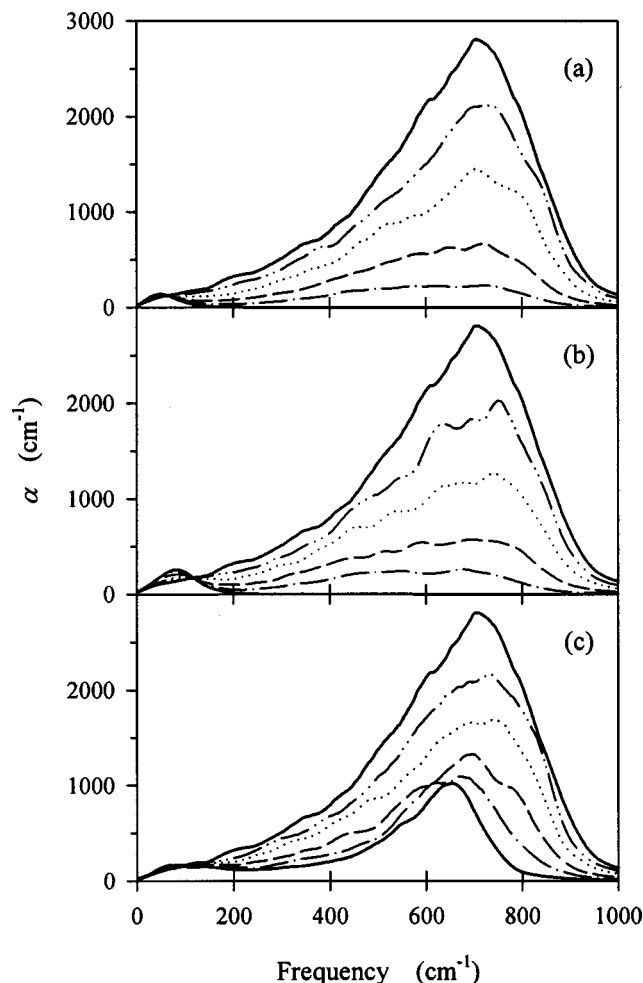


FIG. 6. The simulated total dipole spectra of (a) acetone/water, (b) acetonitrile/water, and (c) methanol/water mixtures. The line types and compositions are the same as in Fig. 4.

integrating the normalized single dipole ACF:

$$\tau_S^i = \int_0^\infty \langle \mu_i(0) \cdot \mu_i(t) \rangle / \mu_i^2 dt, \quad (5)$$

where  $\mu_i$  is the molecular dipole of species  $i$ . The acetone and acetonitrile single particle ACFs change regularly on dilution, but in opposite directions: acetone molecules relax more lethargically in the presence of water, whereas acetonitrile molecules relax slightly more rapidly. These changes in the ACFs are reflected in minor red- and blue-shifts in the single particle spectra (not shown) of acetone and acetonitrile. Methanol molecules relax faster in water-rich compositions.

The relaxation of individual water molecules becomes increasingly sluggish with dilution. In methanol/water mixtures, the single particle ACFs of water and methanol have similar values at all compositions — that is, the water molecule ACF is similar to that of methanol at methanol-rich compositions, and vice versa. Both methanol and water show a significant blue-shift in the single particle spectra with increasing methanol content (Fig. 9), as Ladanyi and Skaf have

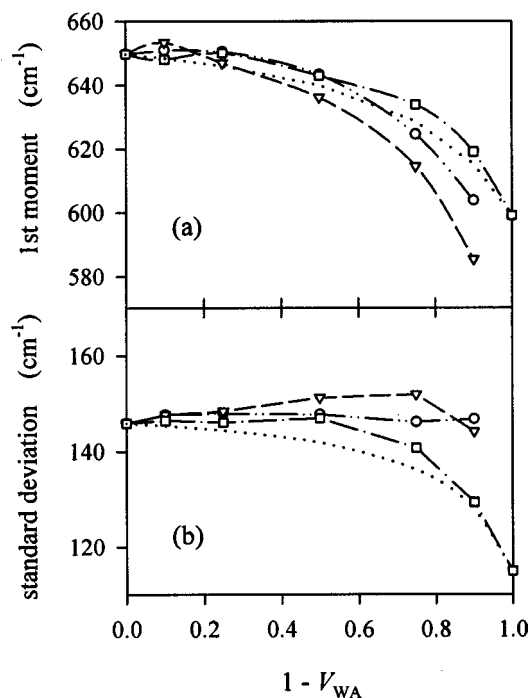


FIG. 7. The composition dependence of the (a) first moment and (b) standard deviation of the spectra in Fig. 6, over the range 300 to 950  $\text{cm}^{-1}$ . For ideal mixtures of acetone/water (open circles and dash-dot-dotted lines) and acetonitrile/water (open triangles and dashed lines), these values do not change with composition. In methanol/water mixtures (open squares and dash-dotted lines), however, the ideal behavior does depend on composition (dotted line).

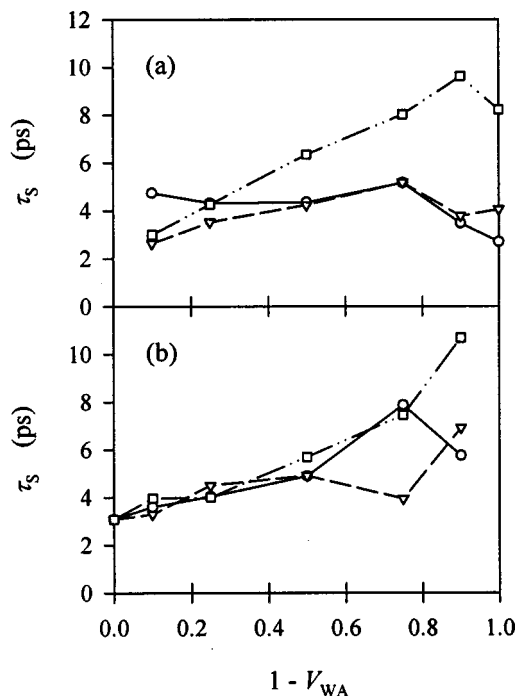


FIG. 8. The single dipole relaxation times of (a) the co-solvent and (b) the water molecules. Relaxation times in acetone/water mixtures are shown as circles and solid lines, those in acetonitrile/water mixtures as triangles with dashed lines. Relaxation times of methanol/water mixtures are given by squares and dash-dot-dotted lines.

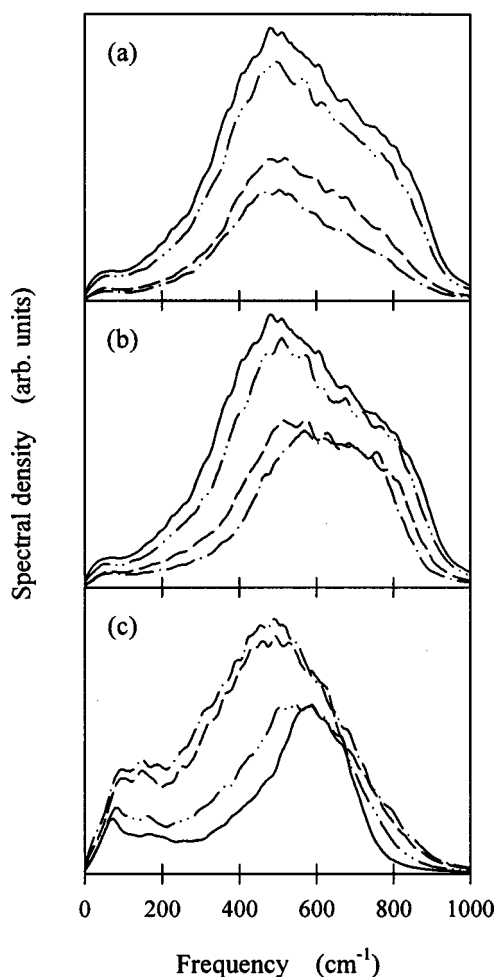


FIG. 9. The single molecule spectra of (a) water in acetone/water mixtures and (b) water and (c) methanol in methanol/water mixtures. Compositions shown (by volume fraction of the displayed species) are 1.00 (solid line), 0.75 (dash-dot-dotted line), 0.25 (dashes), and 0.10 (dash-dotted line).

found.<sup>23</sup> In contrast, single molecule spectra of water in acetone and acetonitrile are relatively unaffected by mixing [Fig. 9(a)].

Changes in the linear velocity ACFs and their spectra are small in the mixtures considered in this study. Compared to neat water, the linear velocity ACFs of water molecules are marginally slower in the mixtures, and become more oscillatory in methanol-rich mixtures.

The angular velocity ACFs of acetone decay faster, and those of acetonitrile decay slower, with the addition of water. These changes are reflected in small shifts in the spectra to higher and lower frequencies, respectively. The angular velocities of water molecules (Fig. 10) are unaffected by the addition of acetone or acetonitrile until low water concentrations, when a small red-shift appears. Kovacs and Laaksonen have observed similar behavior.<sup>4</sup> Larger changes are apparent in the methanol/water mixtures, and both species are more oscillatory at methanol-rich mixtures. The angular velocity spectra of both methanol and water molecules are generally narrower and blue-shifted at methanol-rich compositions.

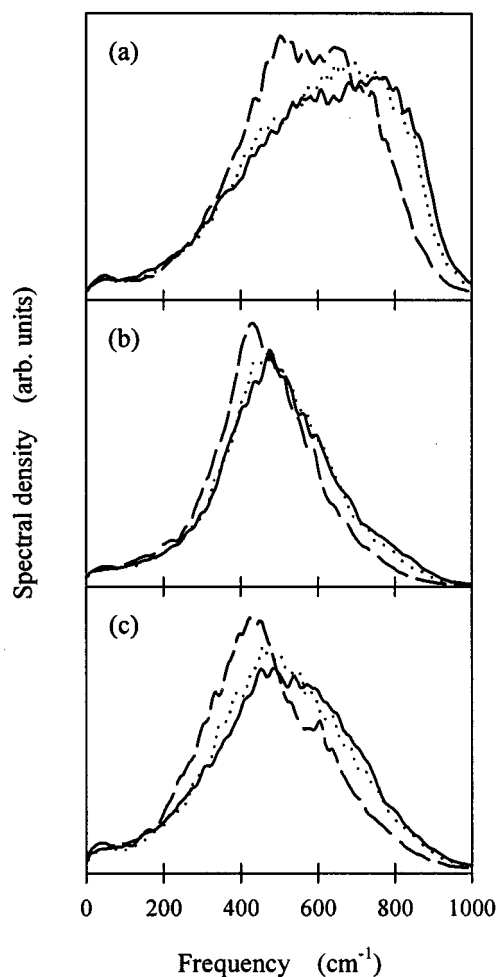


FIG. 10. The angular velocity spectra of the water molecule in acetonitrile/water mixtures: (a)  $\omega_x$ , (b)  $\omega_y$ , and (c)  $\omega_z$ . The water molecule lies in the  $x$ - $z$  plane with its dipole along the  $z$ -axis. The compositions shown are neat water (solid lines), 0.50 (dotted lines), and 0.90 (dashed lines) by acetonitrile volume fraction.

## 2. Hydrogen bonding

The hydrogen bonding state of each molecule in the simulation was categorized at each output configuration. Although the hydrogen bonding of aqueous mixtures has been described before,<sup>20,54</sup> here we present the fractions of molecules in each *unique* hydrogen bonding state. The bonding states of methanol and water are denoted by  $xd_i-ya_j$ , where  $x$  is the number of hydrogen bonds donated to species  $i$ , and  $y$  is the number of bonds accepted from species  $j$ . Water can donate up to two hydrogen bonds, whereas methanol can only donate one. Hydrogen bonds were evaluated according to the usual geometric criteria:<sup>54,55</sup> for hydrogen bond accepting atom,  $Z$ , a hydrogen bond was assigned if  $r_{Z-H} < 2.6$  Å,  $r_{Z-O} < 3.5$  Å, and the H-O... $Z$  angle was less than  $30^\circ$ . These values correspond approximately to the first minimum of the appropriate RDF of the systems being studied. Aqueous mixtures of acetone and acetonitrile will be considered together before hydrogen bonding in the methanol/water mixtures is discussed.

Hydrogen bonding in the acetonitrile/water system has previously been studied by Bertie and Lan using IR spectroscopy,<sup>56</sup> and by Bergman and Laaksonen using MD



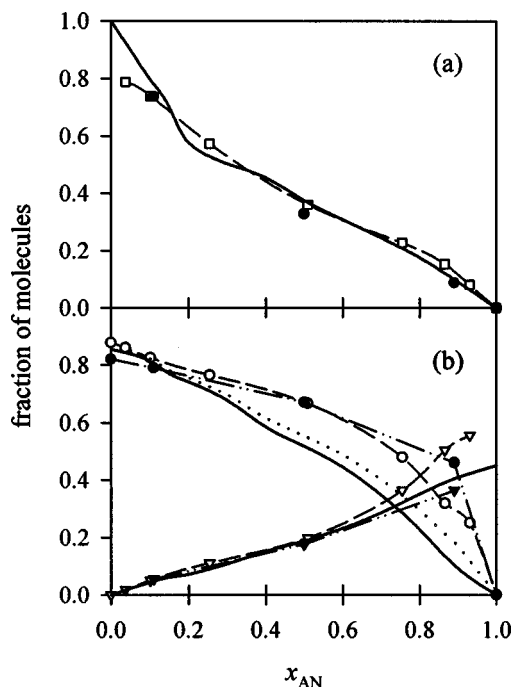


FIG. 11. (a) The fraction of acetonitrile molecules that are hydrogen bonded. The solid line is from Bertie and Lan (Ref. 56), filled circles are from Bergman and Laaksonen (Ref. 57), and our results are shown by open squares and a thin dashed line. (b) The fraction of water hydrogen atoms donated to water (circles) and to acetonitrile (triangles) molecules. The Bertie results are again shown as a bold solid line. The Bertie results based on values at one standard deviation are shown by the dotted line. In this and the following figures, lines through the points are intended as guides to the eye.

simulations with SPC/E water.<sup>57</sup> Their results and ours are shown in Fig. 11. The simulations show good agreement with the spectroscopic determination of the fraction of hydrogen bonded acetonitrile molecules, and with the fraction of water hydrogen atoms that are donated to acetonitrile. At high acetonitrile compositions, our results suggest slightly more, and those of Bergman and Laaksonen suggest fewer, hydrogen bonds to acetonitrile. More substantial differences are evident when considering the fraction of protons donated to other water molecules. The simulations show more hydrogen bonding between water molecules than do the spectroscopic results. The discrepancy in this regard is more marked in the results of Bergman and Laaksonen, possibly because they scale the self-energy term of the SPC/E model with composition. We note that the results of Bertie and Lan depend on the assignment of the absorption bands of each type of OH stretch, and that their results at one standard deviation are significantly closer to ours [dotted line in Fig. 11(b)]. Nevertheless, the experimental data suggest that the simulations exaggerate the extent of hydrogen bonding between water molecules. With this in mind, we proceed to a more detailed analysis of hydrogen bonding in the mixtures.

The average number of hydrogen bonds to water and its co-solvent is shown in Fig. 12(a) for acetone/water (filled symbols and dashed lines) and acetonitrile/water mixtures (open symbols and solid lines). As has been observed before,<sup>20</sup> the number of hydrogen bonds donated by water is largely constant as a function of composition. Similar behavior was observed in the number of bonds donated by metha-

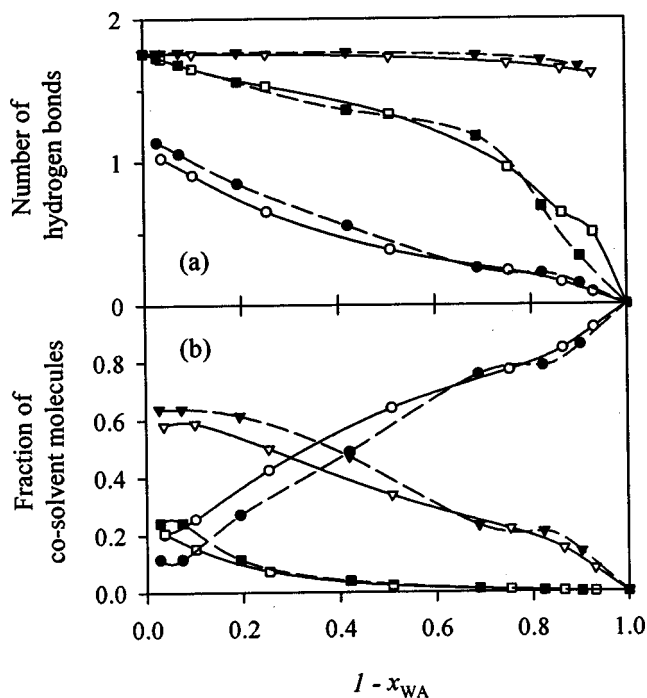


FIG. 12. (a) The average number of hydrogen bonds in acetone/water and acetonitrile/water mixtures. The average number of hydrogen bonds donated (triangles) and accepted (squares) by water molecules, and the average number of bonds accepted by the co-solvent (circles), are shown. (b) The fraction of co-solvent molecules accepting zero (circles), one (triangles), or two (squares) hydrogen bonds. In both (a) and (b), acetone mixtures are designated by closed symbols and dashed lines, and acetonitrile mixtures by open symbols and solid lines.

nol in mixtures with acetone and acetonitrile.<sup>7</sup> The number of hydrogen bonds that water accepts (squares) is insensitive to the identity of the co-solvent except at low water concentrations, where differences between the two systems become noticeable. Rather than decreasing linearly to zero, the number of hydrogen bonds accepted by water displays a convex dependence on composition, thereby proving that water molecules aggregate together rather than mixing randomly. In both systems, water molecules are least randomly mixed at about  $x_{WA} \approx 0.3$ . Acetonitrile (open circles) forms fewer hydrogen bonds with water than does acetone (filled circles) at water-rich compositions. Slight differences are apparent in the fractions of acetone and acetonitrile molecules in each bonding state [Fig. 12(b)]. The bonding state of acetonitrile molecules (open symbols) changes fairly smoothly with composition, whereas acetone molecules (filled symbols) have a plateau at  $0.7 < x_{AT} < 0.8$  and below  $x_{AT} = 0.10$ .

The hydrogen bonding states of the water molecules in acetone/water and acetonitrile/water mixtures are shown in Figs. 13 and 14. Part (a) of these figures shows water hydrogen bonding states involving exclusively one species, whereas (b) shows states where the water molecule is hydrogen bonded to both species. Low concentrations of acetone and acetonitrile ( $x_{AT}, x_{AN} < 0.20$ ) have an identical effect on water hydrogen bonding, but differences between acetone and acetonitrile mixtures arise upon further dilution of water. These differences are subtle and appear to be primarily related to the strength of hydrogen bonding between water and

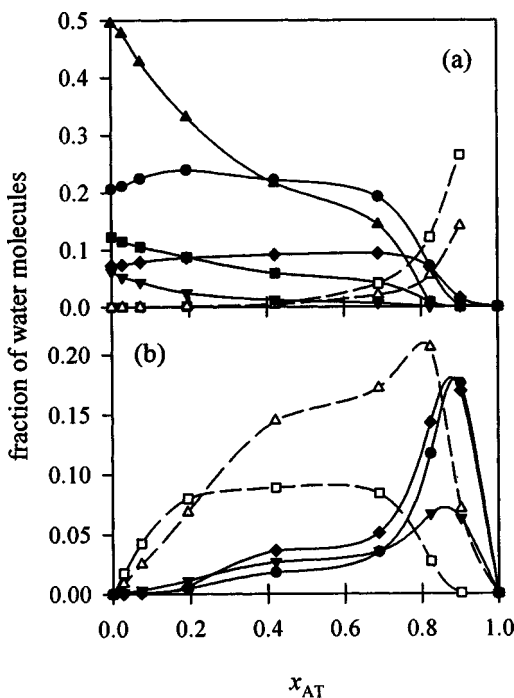


FIG. 13. The fraction of water molecules in different hydrogen bonding states in acetone/water mixtures. (a) Hydrogen bonding states involving only water (solid lines) or only acetone (dashed lines) molecules:  $2d_{WA}-2a$  (filled upward pointing triangles),  $2d_{WA}-1a$  (filled circles),  $1d_{WA}-2a$  (filled squares),  $1d_{WA}-1a$  (filled diamonds),  $2d_{WA}-3a$  (filled downward pointing triangles),  $2d_{AT}-0a$  (open squares), and  $1d_{AT}-0a$  (open triangles). In (b) are shown states involving both species:  $1d_{AT}1d_{WA}-0a$  (filled circles),  $1d_{AT}-1a$  (filled triangles),  $2d_{AT}-1a$  (filled diamonds),  $1d_{AT}1d_{WA}-2a$  (open squares), and  $1d_{AT}1d_{WA}-1a$  (open triangles).

its co-solvent. The remarkable retention of water connectivity in the mixtures is evident in part (a) of the figures, particularly in the tetrahedrally bonded water molecules ( $2d_{WA}-2a$ —filled upward-pointing triangles). The high connectivity between water molecules is also retained in molecules with three hydrogen bonds ( $2d_{WA}-1a$ —filled circles, and  $1d_{WA}-2a$ —filled squares), to the extent that in acetone/water mixtures up to  $x_{AT}=0.70$ , most water molecules are still exclusively hydrogen bonded to other water molecules.

The hydrogen bonding between water molecules in the acetone/water system changes dramatically at about  $x_{AT}=0.70$ , when the fraction of water molecules that are hydrogen bonded to two or more other water molecules drops rapidly. Above  $x_{AT}=0.80$ , few water molecules are hydrogen bonded to more than two other water molecules. The loss of water connectivity is more gradual in acetonitrile/water mixtures (Fig. 14), and a significant fraction of water molecules remains hydrogen bonded to two or three other water molecules at acetonitrile-rich compositions. Hydrogen bonding between water and its co-solvent predominates at low water concentrations, and the number of water molecules bonded exclusively to the co-solvent ( $2d_{AT,AN}-0a$ , open squares, or  $1d_{AT,AN}-0a$ , open triangle) increases rapidly below  $x_{WA}=0.20$ . This effect is more marked in the acetone/water mixtures.

The hydrogen bonding statistics of methanol/water mix-

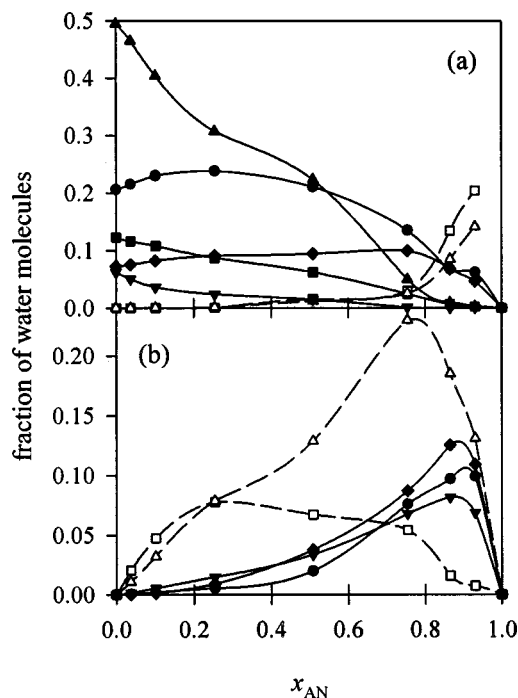


FIG. 14. The fraction of water molecules in different hydrogen states in acetonitrile/water mixtures. The states shown are the same as those in Fig. 13, except that hydrogen bonds are donated to acetonitrile molecules in this figure. For instance, the filled circles in (b) of this figure denote  $1d_{AN}1d_{WA}-0a$ , rather than  $1d_{AT}1d_{WA}-0a$ .

tures are shown in Fig. 15. This system exhibits a higher degree of randomization than in the previous mixtures, as manifest by the positions of the maxima of methanol molecules that are bonded to both species. In Fig. 15(b), for instance,  $1d_{ME}-1a_{WA}$  (filled triangles) and  $1d_{WA}-1a_{ME}$  (open squares) have maxima that are not too far from  $x_{ME}=0.50$ , and the maxima of  $1d_{WA}-1a_{ME}1a_{WA}$  (filled squares) and  $1d_{ME}-2a_{WA}$  (open circles) are near  $x_{ME}=0.33$ , as expected for randomly mixed molecules. Adding water to methanol rapidly reduces the fraction of middle-of-chain [ $1d_{ME}-1a_{ME}$ —open circles in part (a)] methanol molecules. In like manner, the fraction of methanol molecules that have three hydrogen bonds to water [ $1d_{WA}-2a_{WA}$ —filled squares in (a)] increases sharply as the methanol content decreases. This accords with work by other researchers who have found that methanol becomes water-like in its bonding characteristics in water-rich mixtures.<sup>21,22</sup>

There are too many unique hydrogen bonding states of water molecules in methanol/water mixtures to present meaningfully here.<sup>58</sup> Our analysis was therefore simplified by considering only the total number of hydrogen bonds to each species. The water bonding state is designated by  $i_{ME}-j_{WA}$ , where  $i$  and  $j$  are the total number of hydrogen bonds to methanol and to water. The most prominent species are shown in Fig. 16. Water molecules tend to bond preferentially to other water molecules. Consequently, the fractions of water molecules bonded to both species have maxima at compositions higher in methanol than expected for randomly dispersed molecules. This effect is illustrated in Fig. 17, where water molecules bonded exclusively to other water molecules are shown. If mixing occurs randomly, then the

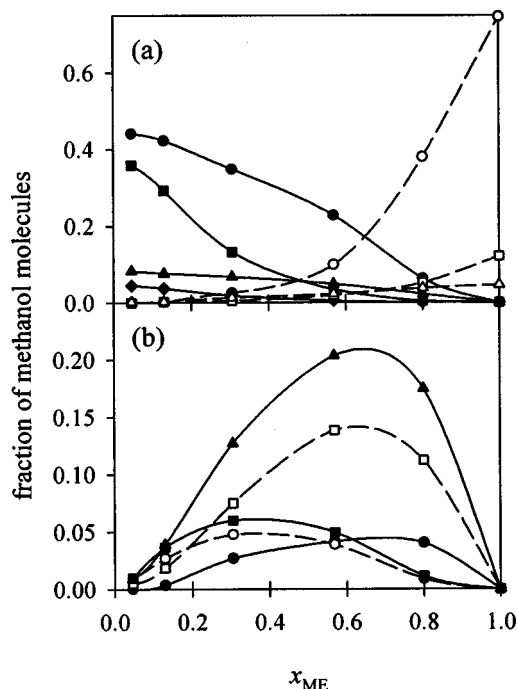


FIG. 15. The fraction of methanol molecules in different hydrogen bonding states in methanol/water mixtures. Hydrogen bond states involving only methanol (dashed lines) or only water (solid lines) molecules are shown in (a):  $1d_{WA}-1a_{WA}$  (filled circles),  $1d_{WA}-2a_{WA}$  (filled squares),  $0d-1a_{WA}$  (filled triangles),  $0d-2a_{WA}$  (filled diamonds),  $1d_{ME}-1a_{ME}$  (open circles),  $1d_{ME}-0a$  (open squares), and  $0d-1a_{ME}$  (open triangles). States involving both species are shown in (b):  $1d_{ME}-1a_{ME}2a_{WA}$  (filled circles),  $1d_{ME}-2a_{WA}$  (open circles),  $1d_{WA}1a_{ME}$  (open squares),  $1d_{WA}-1a_{ME}1a_{WA}$  (filled squares), and  $1d_{ME}-1a_{WA}$  (filled triangles).

probability,  $p$ , of being hydrogen bonded to exactly  $n$  water molecules can be estimated by  $p = p_0^* x_{WA}^n$ , where  $p_0$  is the probability in neat water. This estimate does not take into account how the total number of hydrogen bonds to the water molecule changes with composition, i.e.,  $p_0$  is assumed to be independent of composition. In fact, because the number of molecules in water's solvation shell decreases in methanol mixtures, the probability of randomly finding four hydrogen bonding species should be even lower than that shown. Figure 17 shows that water molecules are more likely to associate with themselves than expected for completely random mixing. Similar considerations applied to the hydrogen bonding states in mixtures with acetone and acetonitrile demonstrate that these mixtures are even less randomly mixed.

### 3. Spatial distribution functions

Our SDFs of the acetonitrile/water and methanol/water systems are in broad agreement with those of Laaksonen and co-workers.<sup>21,57</sup> Therefore, we shall discuss only the SDFs of acetone/water mixtures, which have not yet been described in the literature. We shall focus on the position of the oxygen atoms,  $O_{AT}$  and  $O_{WA}$ , relative to the acetone and water molecules (Fig. 18).

The water- $O_{WA}$  SDFs show the usual tetrahedral structure of water in water-rich mixtures [Fig. 18(a)], and secondary structure is visible at low isosurface values. Dilution of

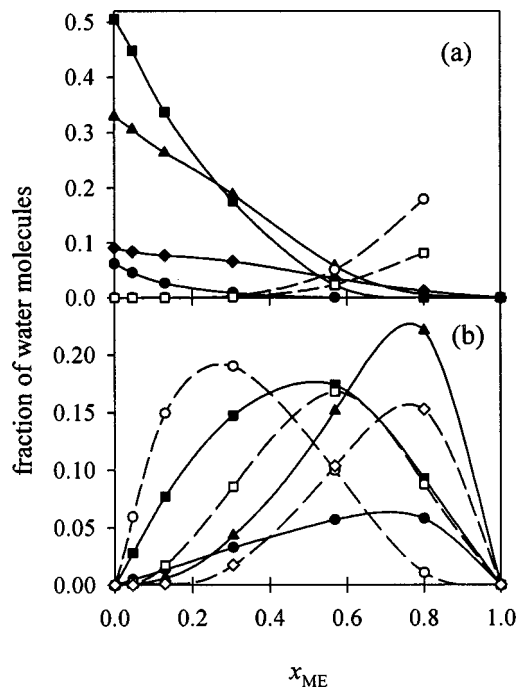


FIG. 16. The fraction of water molecules in different hydrogen bonding states in methanol/water mixtures. (a) Hydrogen bond states involving only water (solid lines) or methanol (dashed lines) molecules:  $0_{ME}5_{WA}$  (filled circles),  $0_{ME}4_{WA}$  (filled squares),  $0_{ME}3_{WA}$  (filled triangles),  $0_{ME}2_{WA}$  (filled diamonds),  $4_{ME}0_{WA}$  (open squares), and  $3_{ME}0_{WA}$  (open circles). In (b) are states involving both species:  $1_{ME}1_{WA}$  (filled circles),  $1_{ME}2_{WA}$  (filled squares),  $1_{ME}3_{WA}$  (open circles),  $2_{ME}1_{WA}$  (filled triangles),  $2_{ME}2_{WA}$  (open squares), and  $3_{ME}1_{WA}$  (open diamonds).

water with acetone results in a large increase in the SDF values, indicating that water molecules tend to remain in hydrogen bonded clusters. The tetrahedral position of the hydrogen bond donors to the water molecule is gradually lost to a more dipolar position [Fig. 18(b)], and secondary structure is no longer visible. The water- $O_{AT}$  SDFs (not shown) are found almost exclusively in the hydrogen bond accepting position, with no other prominent features visible. The maximum value of the SDFs increases significantly in acetone-

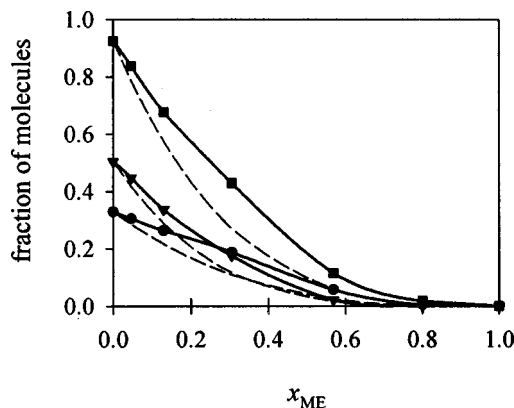


FIG. 17. The fraction of molecules of water that are hydrogen bonded exclusively to other water molecules:  $0_{ME}3_{WA}$  (filled circles) and  $0_{ME}4_{WA}$  (filled triangles). For comparison, an estimate of random mixing for each state is shown as thin dashed lines. The sum of the most prominent species in neat water ( $0_{ME}2_{WA} + 0_{ME}3_{WA} + 0_{ME}4_{WA}$ ), and of the random estimates of these states are also shown (filled squares).

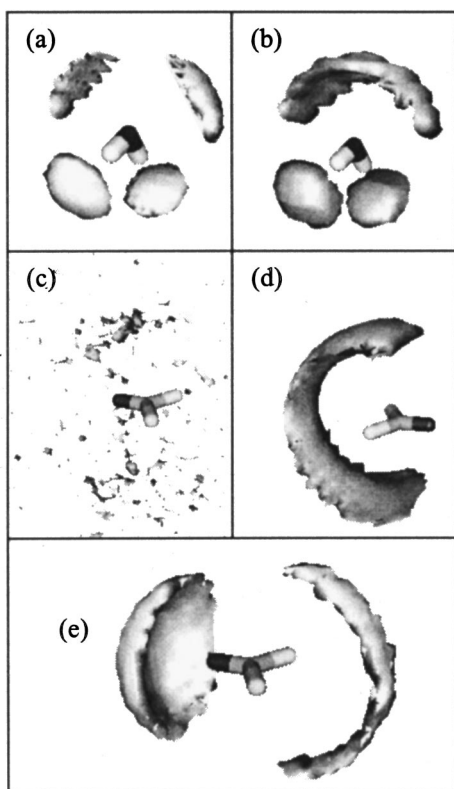


FIG. 18. The SDFs of the acetone/water mixtures. The isosurface values,  $a$ , and maxima,  $b$ , in the SDFs are denoted as  $(a/b)$ . Water- $O_{WA}$  at (a)  $V_{AT} = 0.10$  (4/38) and (b) 0.95 (15/162). Acetone- $O_{AT}$  at (c)  $V_{AT} = 0.10$  (10/27) and (d) 0.90 (2/5). Acetone- $O_{WA}$  is shown in (e) for  $V_{WA} = 0.90$  (2/5). The darkest site of the central molecule is the oxygen atom for both species.

rich mixtures, signifying that water molecules are more dispersed in acetone-rich mixtures and donate a greater number of hydrogen bonds to acetone.

The high SDF values of  $O_{AT}$  sites relative to acetone molecules indicate that acetone molecules aggregate in water-rich mixtures. However, there is no preferred orientation for these sites relative to the acetone molecule, probably because their positions are dictated by the water structure [Fig. 18(c)]. At high acetone concentrations, the  $O_{AT}$  site lies in a crescent behind the  $C=O$  bond [Fig. 18(d)].  $O_{WA}$  sites have no preferred position to acetone molecules at low acetone concentrations—the water molecules seem to have little interaction with the solute and the water structure is relatively unperturbed. At higher concentrations of acetone, the  $O_{WA}$  molecules are more localized in the hydrogen bond donating site, and in a crescent similar to that of  $O_{AT}$  [Fig. 18(e)].

## V. DISCUSSION

Simulated spectra reproduce the most important features in the experimental spectra of the mixtures, and show good agreement with the compositional dependence of the experimental spectra. These include the blue-shift of methanol/water mixtures (relative to ideal behavior) over the whole composition range, the slight blue-shifts of the spectra at low concentrations of acetone and acetonitrile, and the red-shifts at high concentrations of acetone and acetonitrile. The red-

shifts of the simulated spectra are not quite as large as those of the experimental spectra. The simulated peak widths are in fair agreement with the experimental spectra. We believe that this is the first comparison of the experimental and computed spectra of these mixtures. The broad agreement in the compositional trends of the spectra is most pleasing, and gives us confidence that the simulations accurately model the most important aspects of the dynamics of the mixtures.

The Debye relaxation times based on the far-IR spectra agree with results obtained at microwave frequencies. This relaxation time describes the relaxation of the orientational polarization—that is, the collective rotational diffusion of the sample. The relaxation times are slower than those of ideal mixtures, which is reflected in the absorption coefficients of the real mixtures being smaller than those of ideal mixtures. The observed changes in the absorption coefficient of the mixtures in the far-IR cannot be attributed to shifts in the water librational bands because these bands occur at much higher frequencies, nor to changes in the co-solvent librational bands since these are relatively unaffected by mixing.

Skaf and Ladanyi have shown convincingly that the slowing of the rotational diffusional motion in methanol/water and DMSO/water mixtures is strongly affected by the collective *interspecies* cross-correlation, which is the slowest contribution to the dipole moment of the system.<sup>12,23</sup> The collective relaxation of molecules of the same species is also slower than that of individual molecules. Their results suggest an anticooperative effect in the reorientational motions in the liquid that is somewhat more pronounced between molecules of different species than between those of the same species. We expect that the same effect is responsible for the slower rotational diffusional dynamics that we find in the systems studied here.

The observed slowing of the collective dynamics of the mixtures is probably caused by changes in hydrogen bonding, since these bonds are responsible for the associating nature of water. A possible mechanism for such a change might be related to the substitution of four hydrogen bonded states of water molecules with two and three hydrogen bonded states. By so doing, the hydrogen bonding character of water increasingly resembles that of methanol in which two hydrogen bonded molecules predominate. The exceptionally long-lived nature of methanol molecules in the  $1d_{ME}-1a_{ME}$  state compared to those in other states,<sup>59</sup> and the sluggish dynamics of methanol chains, make reorientation a slow process. We propose that the extent to which water becomes more chain-like is reflected in more sluggish rotational dynamics in the system. Other workers have found that water molecules assemble in chains and loops at low concentrations.<sup>57</sup>

There is a substantial discrepancy between the high frequency behavior of individual water molecules and that of the entire system, as indicated by the single particle spectra and the total dipole spectra. This suggests that an explanation similar to that presented earlier is also applicable to the high frequency behavior—namely, that there are significant differences between the single particle ACFs and collective cross-correlation TCFs. At high frequencies, however, the interspecies cross-correlations are not expected to play much



of a role, because there is no inertial contribution to their spectra.<sup>12,23</sup> Consequently, the observed high frequency behavior in the total dipole spectra is primarily due to collective motions of water molecules (and also to the collective motions of methanol molecules in methanol/water mixtures). The collective behavior of water molecules has significantly more high frequency components than single water molecules. In contrast, the collective high frequency behavior of neat methanol seems to reflect the behavior of individual methanol molecules, as the single particle spectrum of methanol coincides much more closely with the spectrum of the whole system.<sup>7</sup> The effect of mixing on the total dipole spectra is also reflected in the single dipole spectra of methanol molecules. High frequency cooperative effects therefore appear to be less important in methanolic than in aqueous systems.

The effect that acetone and acetonitrile have on the high frequency behavior of aqueous mixtures differs substantially from that of methanol. Differences are also evident in the single particle behavior and in the effect of the co-solvent on the hydrogen bonding environment of the mixtures. Therefore, we will examine aqueous mixtures of acetone and acetonitrile together and discuss methanol/water mixtures separately.

The high frequency dynamics of individual water molecules in acetone/water and acetonitrile/water mixtures are largely unaltered over most of the composition range. The changes in the dynamics of water molecules are modest, even when dilute. In particular, the angular velocities of water molecules are negligibly affected by mixing for  $V_{WA} > 0.25$ , and only relatively small red-shifts are seen at  $V_{WA} = 0.10$ . Furthermore, the single particle spectra of water are not shifted at all by mixing (although the intensity of the spectrum decreases). These results must be reconciled with the observation that the high frequency dynamics of the total dipole of the system (in simulated and experimental spectra) displays marked changes on mixing.

The usual explanation for the above observations would be in terms of the hydrogen bond strengths and the water structure of the mixtures. Accordingly, a blue-shift indicates a strengthening in the structure or hydrogen bonding environment of the liquid, and a red-shift indicates a weakening in the interaction between molecules. Thus, in the acetonitrile/water system, Kovacs and Laaksonen have proposed that the red-shift of the angular velocity spectra of water molecules arises from fewer and weaker hydrogen bonds, and signifies a breakdown of the hydrogen bonding structure.<sup>4</sup> However, the angular velocity and single dipole spectra change little, whereas a weakening in the hydrogen bonding of water molecules should manifest itself in changes to the single dipole spectrum.

An increase in the structure of the liquid might explain the small blue-shift that occurs upon addition of small amounts of acetone or acetonitrile. However, it is difficult to reconcile an increase in structure with the observed changes in hydrogen bonding, particularly the decrease in the concentration of the quintessentially structured water molecule ( $2d_{WA} - 2a$ ) that occurs immediately on mixing. Harris and Nevitt have observed, based on the pressure dependence of

the diffusion coefficient, that there is no evidence for structural enhancement in the acetonitrile/water mixture.<sup>60</sup> For these reasons, describing frequency shifts in the water librational band in terms of hydrogen bond strength and liquid structure does not adequately explain the observed dynamical behavior.

The relatively unaffected spectra of the individual molecules, in contrast to the red-shifts observed in the total dipole moment, indicate that mixing principally affects the *collective* motions in the liquid. The results presented here therefore suggest that the co-solvent enhances the high-frequency collective motions slightly in water-rich mixtures, but decreases them at low water concentrations. As described earlier, the largest influence on the high frequency spectra is likely to be cross-correlations between molecules of the same species, since interspecies cross-correlations do not have a large high frequency component arising from inertial contributions. The shift to lower frequencies is most apparent at  $V_{WA} \leq 0.25$ , which is concomitant with the loss of significant water connectivity. The collective behavior of water therefore becomes more like that of individual water molecules. The observation that the red-shift is even larger in experimental spectra suggests that there may be a greater loss of connectivity in real water than indicated by the simulations.

The primary differences between acetone and acetonitrile as co-solvents are probably related to the strength of the hydrogen bonds that they form with water. The correct representation of hydrogen bonding between water and its co-solvent is therefore essential to simulate the mixtures accurately. The larger red-shift observed in acetonitrile than in acetone mixtures is probably due to the lower water connectivity in acetonitrile/water mixtures for  $V_{WA} \geq 0.10$ . Furthermore, in the low water concentration regime, we expect the strength of hydrogen bonding between water and its co-solvent to significantly influence the resulting spectra. The ability of acetone to form relatively strong hydrogen bonds to water would allow water molecules to be dispersed more readily in acetone-rich mixtures, and thereby result in the loss of high water connectivity. On the other hand, water molecules in acetonitrile/water mixtures retain a higher level of connectivity to other water molecules when dilute, and changes in the hydrogen bonding environment occur more gradually. Water clusters are therefore more likely to be formed in acetonitrile than in acetone mixtures, and clusters have indeed been inferred at low water concentrations in acetonitrile/water mixtures.<sup>4,61</sup>

The retention of high water connectivity on dilution with acetone or acetonitrile is remarkable. Tetrahedrally bonded water molecules ( $2d_{WA} - 2a$ ) exist over a much larger composition range than expected of a random mixture. The loss of tetrahedrally bonded water is compensated for by an increase in the number of triply hydrogen bonded water molecules, which are relatively common up to low concentrations of water. Nevertheless, it does not seem appropriate to describe the water structure as *increasing* on mixing, if the structuredness in water is based on how tetrahedral the water is, since the co-solvent does not make the water more tetrahedral. This assessment from the simulations agrees with the compelling experimental evidence of Harris and Newitt.<sup>60</sup>

Therefore, the increases that have been observed in the lifetimes of water–water and water–co-solvent hydrogen bonds are probably more related to the slowing of collective and cooperative motions in the liquid than to changes in the structure of the environment.<sup>20,54</sup> The loss of four hydrogen bonded water molecules on mixing has been reported.<sup>20</sup> Only at high concentrations of acetone or acetonitrile do water molecules form significant numbers of hydrogen bonds to the co-solvent, reflected especially in the sharp peaks found in acetone/water mixtures for  $x_{AT} > 0.8$ . The sharp peaks in  $1d_{AT}1d_{WA}-0a$  and  $2d_{AT}-1a$  in Fig. 13 suggest that acetone molecules compete effectively for hydrogen bonds only at low water concentrations.

Our results for the fraction of hydrogen bonded water and acetonitrile molecules are in fair agreement with the experimentally inferred values of Bertie and Lan.<sup>56</sup> Although there is some uncertainty in their values, it appears that the simulations overstate water–water bonding. Water–acetonitrile hydrogen bonds may also be too common in the simulations of acetonitrile-rich mixtures.

Methanol differs from acetone and acetonitrile in that it also functions as a hydrogen bond donor, thereby facilitating its incorporation into the water network. Likewise, water molecules fit into the methanol network easily. In both cases, the solute adopts some of the hydrogen bonding character of the solvent.<sup>21,22</sup> The mixing of molecules of these two liquids is not entirely random, however, and there is a fair amount of self-association, although less so than in acetone and acetonitrile mixtures.

The dynamics of methanol and water molecules resemble each other over all compositions, as has been observed in the literature.<sup>23</sup> This is reflected in the single particle time constants of methanol and water molecules, which have similar values over the whole composition range. Furthermore, the librational spectra of both molecules occur at lower frequencies in water-rich mixtures, and progressively shift to higher frequencies in methanol-rich mixtures. Similar trends are observed in the high frequency angular velocity spectra of the mixtures. The similarities in the dynamics of both molecules are consistent with the similarity in structure. The blue-shift of the total dipole spectra of the mixtures is probably a result of relatively strong hydrogen bonds from water to methanol, and their influence on the collective high frequency behavior of the liquid. A similar blue-shift was observed in DMSO/water mixtures, in which the water–DMSO hydrogen bond is known to be stronger than that between water molecules.<sup>12</sup>

## VI. CONCLUSIONS

Binary mixtures of acetone/water, acetonitrile/water, and methanol/water mixtures have been investigated over the whole composition range. Far-IR spectra of the mixtures absorb substantially less than calculated for ideal mixtures, which is reflected in the slower orientational relaxation of the mixtures. Infrared spectra of acetone and acetonitrile mixtures with water are similar, exhibiting a slight blue-shift as the co-solvent is added to water, followed by a large red-shift

at high co-solvent concentrations. Spectra of methanol/water mixtures are blue-shifted over their whole composition range.

Simulated spectra from MD simulations reproduce the compositional dependence of the experimental spectra. Minor changes are observed in the angular velocity and single dipole spectra of acetone/water and acetonitrile/water mixtures. The red-shift of the total dipole was explained in terms of changes in the collective behavior of the mixtures. In mixtures of methanol and water, on the other hand, molecules of both species exhibit similar dynamical behavior, changing monotonically from water-like dynamics at water-rich compositions, to methanol-like dynamics at methanol-rich compositions.

The hydrogen bonding in the mixtures was examined in greater detail than has been done previously. The tetrahedral structure of water is lost as the co-solvent concentration increases, but three and two hydrogen bonded water molecules remain over an extensive range of compositions. Water molecules have a tendency to aggregate in all of the mixtures, but in acetone and acetonitrile mixtures this tendency was especially marked. The detailed evaluation of the static connectivity of water molecules is only a first step towards understanding the water hydrogen bonding network. By evaluating how the hydrogen bonding network changes in time, it should be possible to broaden our knowledge of *cooperative* motions in water. Work towards this end is currently being pursued.

## ACKNOWLEDGMENT

Support from a National Science Foundation CAREER award (CHE-9703432) is gratefully acknowledged.

- <sup>1</sup>E. v. Goldammer and H. G. Hertz, J. Phys. Chem. **74**, 3734 (1970).
- <sup>2</sup>H. S. Frank and M. W. Evans, J. Chem. Phys. **13**, 507 (1945).
- <sup>3</sup>Y. I. Naberukhin nad A. Rogov, Russ. Chem. Rev. **40**, 297 (1971).
- <sup>4</sup>H. Kovacs and A. Laaksonen, J. Am. Chem. Soc. **113**, 5596 (1991).
- <sup>5</sup>B. M. Ladanyi and M. S. Skaf, Annu. Rev. Phys. Chem. **44**, 335 (1993).
- <sup>6</sup>D. S. Venables, A. Chiu, and C. A. Schmuttenmaer, J. Chem. Phys. **113**, 3243 (2000).
- <sup>7</sup>D. S. Venables and C. A. Schmuttenmaer, J. Chem. Phys. **113**, 3249 (2000).
- <sup>8</sup>D. S. Venables and C. A. Schmuttenmaer, J. Chem. Phys. **108**, 4935 (1998).
- <sup>9</sup>J. T. Kindt and C. A. Schmuttenmaer, J. Phys. Chem. **100**, 10373 (1996).
- <sup>10</sup>E. Hawlicka, Pol. J. Chem. **70**, 821 (1996).
- <sup>11</sup>C. Hoheisel, *Theoretical Treatment of Liquids and Liquid Mixtures* (Elsevier, Amsterdam, 1993).
- <sup>12</sup>I. A. Borin and M. S. Skaf, Chem. Phys. Lett. **296**, 125 (1998); M. S. Skaf, J. Phys. Chem. A, **103**, 10719 (1999).
- <sup>13</sup>A. C. Kumbharkhane, S. N. Helambe, M. P. Lakhande, S. Doraiswamy, and S. C. Mehrotra, Pramana, J. Phys. **46**, 91 (1996).
- <sup>14</sup>M. I. Shakhparonov and Y. Y. Akhadov, Zh. Strukt. Khim. **6**, 21 (1965).
- <sup>15</sup>D. Bertolini, M. Cassettari, and G. Salvetti, J. Chem. Phys. **78**, 365 (1983).
- <sup>16</sup>S. Mashino, S. Kuwabara, S. Yagihara, and K. Higasi, J. Chem. Phys. **90**, 3292 (1989).
- <sup>17</sup>U. Kaatze, M. Schäfer, and R. Pottel, Z. Phys. Chem. **165**, 103 (1989).
- <sup>18</sup>J. Timmermans, *The Physico-chemical Constants of Binary Systems in Concentrated Solution*, Vol. 4 (Interscience, New York, 1960).
- <sup>19</sup>N. Micali, S. Trusso, C. Vasi, D. Blaudez, and F. Mallamace, Phys. Rev. E **54**, 1720 (1996).
- <sup>20</sup>M. Ferrario, M. Haughney, I. R. McDonald, and M. L. Klein, J. Chem. Phys. **93**, 5156 (1990).

- <sup>21</sup>A. Laaksonen, P. G. Kusalik, and I. M. Svishchev, *J. Phys. Chem. A* **101**, 5910 (1997).
- <sup>22</sup>G. Pálkás, E. Hawlicka, and K. Heinzinger, *Chem. Phys.* **158**, 65 (1991).
- <sup>23</sup>B. M. Ladanyi and M. S. Skaf, *J. Phys. Chem.* **100**, 1368 (1996).
- <sup>24</sup>H. Tanaka and G. E. Gubbins, *J. Chem. Phys.* **97**, 2626 (1992).
- <sup>25</sup>M. S. Skaf and B. M. Ladanyi, *J. Phys. Chem.* **100**, 18258 (1996).
- <sup>26</sup>G. Pálkás, I. Bakó, K. Heinzinger, and P. Bopp, *Mol. Phys.* **73**, 897 (1991).
- <sup>27</sup>M. S. Skaf and B. M. Ladanyi, *J. Chem. Phys.* **102**, 6542 (1995).
- <sup>28</sup>J. E. Bertie and S. L. Zhang, *J. Chem. Phys.* **101**, 8364 (1994).
- <sup>29</sup>J. E. Bertie and Z. Lan, *Appl. Spectrosc.* **50**, 1047 (1996).
- <sup>30</sup>C. Fattinger and D. Grischkowsky, *Appl. Phys. Lett.* **54**, 490 (1989); P. R. Smith, D. H. Auston, and M. C. Nuss, *IEEE J. Quantum Electron.* **24**, 255 (1988).
- <sup>31</sup>Further optimization of our spectrometer has extended our spectral coverage. Spectra up to  $130\text{ cm}^{-1}$  are now attainable in favorable cases.<sup>6</sup>
- <sup>32</sup>See EPAPS Document No. E-JCPSA6-113-521048 for far-infrared and infrared data. This document may be retrieved via the EPAPS homepage (<http://www.aip.org/pubservs/epaps.html>) or from [ftp.aip.org](ftp://ftp.aip.org) in the directory /epaps/. See the EPAPS homepage for more information. In addition to the data presented in this article, spectra of the nonaqueous mixtures in Ref. 6 have also been archived.
- <sup>33</sup>The MolDy program was coded by K. Refson, and is freely available from the internet at [www.earth.ox.ac.uk/%7Ekeith/moldy.html](http://www.earth.ox.ac.uk/%7Ekeith/moldy.html).
- <sup>34</sup>The difference between the temperatures of the simulation and the experimental spectra is relatively small and is ignored in this article, where the trends in the dynamics as a function of composition are our primary consideration. The simulation temperature of  $25^\circ\text{C}$  is the temperature at which the potentials for the neat liquids were parametrized (see Refs. 35–38).
- <sup>35</sup>W. L. Jorgensen, *J. Phys. Chem.* **90**, 1276 (1986).
- <sup>36</sup>W. L. Jorgensen, J. M. Briggs, and M. L. Contreras, *J. Phys. Chem.* **94**, 1683 (1990).
- <sup>37</sup>W. L. Jorgensen and J. M. Briggs, *Mol. Phys.* **63**, 547 (1988).
- <sup>38</sup>W. L. Jorgensen, J. Chandrasekhar, J. D. Madura, R. W. Impey, and M. L. Klein, *J. Chem. Phys.* **79**, 926 (1983).
- <sup>39</sup>V. S. Griffiths, *J. Chem. Soc.* **1952**, 1326.
- <sup>40</sup>H. Wode and W. Seidel, *Ber. Bunsenges. Phys. Chem.* **98**, 927 (1994).
- <sup>41</sup>V. S. Griffiths, *J. Chem. Soc.* **1954**, 860.
- <sup>42</sup>Two points stand out: (1) the equilibration period is significantly longer than those of numerous earlier studies (Refs. 4, 20, 22, and 26), and (2) the equilibration period depends on which system is being investigated and on the composition of the mixture. The individual molecules require adequate time to explore various configurations within the system, and their (usually) randomly distributed starting positions may be far from equilibrium. The slow relaxation of the RDFs of aqueous mixtures has been noted by Laaksonen *et al.* (Ref. 21).
- <sup>43</sup>B. Guillot, *J. Chem. Phys.* **95**, 1543 (1991).
- <sup>44</sup>D. A. McQuarrie, *Statistical Mechanics* (HarperCollins, New York, 1976).
- <sup>45</sup>A Kramers–Kronig calculation requires the high frequency index of refraction. The indices of refraction for the neat liquids at  $20^\circ\text{C}$  are 1.359 (acetone), 1.344 (acetonitrile), 1.328 (methanol), and 1.333 (water) (Ref. 46). Ideal values of the indices of refraction were used for the mixtures.
- <sup>46</sup>D. R. Lide (ed.), *CRC Handbook of Physics and Chemistry*, 73rd ed. (CRC, Boca Raton, FL, 1992).
- <sup>47</sup>M. Souaille and J. C. Smith, *Mol. Phys.* **87**, 1333 (1996).
- <sup>48</sup>Other models included the Cole–Cole and Cole–Davidson models, the Onsager–Cole, Rocard–Powles and Lobo–Robinson–Rodriguez models, and the Fröhlich, Mori, and Chandra–Wei–Patey models. The Bertolini treatment of the data was also evaluated. See Ref. 49.
- <sup>49</sup>E. Kestemont, F. Hermans, R. Finsy, and R. van Loon, *Infrared Phys.* **18**, 855 (1978); F. Hermans and E. Kestemont, *Chem. Phys. Lett.* **55**, 305 (1978); R. Lobo, J. E. Robinson, and S. Rodriguez, *J. Chem. Phys.* **59**, 5992 (1973); H. Fröhlich, *Theory of Dielectrics* (Clarendon, Oxford, 1986); J. E. Pederson and S. R. Keiding, *IEEE J. Quantum Electron.* **28**, 2518 (1992); A. Chandra, D. Wei, and G. N. Patey, *J. Chem. Phys.* **99**, 2068 (1993); D. Bertolini, M. Cassettari, C. Ferrari, and E. Tombari, *ibid.* **108**, 6416 (1998).
- <sup>50</sup>Y. Y. Akhadov, *Dielectric Properties of Binary Solutions* (Pergamon, New York, 1980).
- <sup>51</sup>T. T. Jones and R. M. Davies, *Philos. Mag.* **28**, 307 (1939).
- <sup>52</sup>Two difficulties arose with analyzing the experimental spectra: (1) Because the Gaussian curve is symmetric, fitting it to the slightly *asymmetric* absorption band of water would result in values of the peak position that are too low. (2) The lower frequency side of the absorption band was inaccessible for some compositions. To handle these difficulties systematically, the curves were fit to as much of the spectra as appeared symmetric. The agreement between the absorption band and the fitted curves over the selected range was good. The fitted values of the peak widths are expected to be slightly low, but should follow changes in the actual peak width.
- <sup>53</sup>For acetone and acetonitrile mixtures, which have no high frequency librations, the ideal peak position and width are the same as those of neat water. The peak positions of methanol and water are almost identical, but the widths differ. Therefore, the ideal peak positions are very similar to those of the neat liquids, whereas the widths change significantly with mixing.
- <sup>54</sup>A. Luzar and D. Chandler, *J. Chem. Phys.* **98**, 8160 (1993).
- <sup>55</sup>J. Marti, J. A. Padró, and E. Guàrdia, *J. Mol. Liq.* **64**, 1 (1995).
- <sup>56</sup>J. E. Bertie and Z. Lan, *J. Phys. Chem. B* **101**, 4111 (1997).
- <sup>57</sup>D. L. Bergman and A. Laaksonen, *Phys. Rev. E* **58**, 4706 (1998).
- <sup>58</sup>For instance, for water molecules that donate up to two and can accept up to three hydrogen bonds, there are 60 unique hydrogen bonding states.
- <sup>59</sup>M. Matsumoto and K. E. Gubbins, *J. Chem. Phys.* **93**, 1981 (1990).
- <sup>60</sup>K. R. Harris and P. J. Newitt, *J. Phys. Chem. B* **103**, 7015 (1999).
- <sup>61</sup>R. D. Mountain, *J. Phys. Chem. A* **103**, 10744 (1999).